Constructing the Universe with Clusters of Galaxies, IAP 2000 meeting, Paris (France) July 2000
Florence Durret & Daniel Gerbal eds.

THE MINIMUM VELOCITY DISPERSION OF VIRIALIZED GALAXY SYSTEMS: A NEW CONSTRAINT ON THE NATURE OF COMPACT GROUPS

G. A. MAMON
Institut d'Astrophysique (CNRS UPR 341), 98 bis Bd Arago, F–75014 Paris, FRANCE (`gam@iap.fr`*)*

Given that a galaxy system must be more massive than its constituent galaxies, the velocity dispersion of a virialized group or cluster of galaxies must be greater than some combination of velocity dispersions of its ellipticals and rotation velocities of its spiral members. Low velocity dispersion systems could either be chance alignments of galaxies within larger systems near cosmological turnaround or alternatively dense systems in the final stages of global coalescence. I compute the minimum velocity dispersion using a stricter criterion than the cosmological $M \sim \sigma_v^3$ relation. I impose that the mass of the system, within any radius that is much larger than the typical inter-galaxy separation is greater than the sum of the masses of its constituent galaxies — if they were isolated — out to that same radius. Adopting the mass profiles that Navarro et al. obtained for structures in cosmological simulations, the minimum velocity dispersion of a group of reasonably massive galaxies obeys $(\sigma_v)^2_{\rm group} \geq 0.5 \sum_E (\sigma_v)^2_E + 0.14 \sum_D v^2_{\rm rot}$, where the sums are over ellipticals (E) and disks (D), and where $v_{\rm rot}$ is the maximum deprojected rotational velocity of a disk galaxy. While internal kinematics data are currently too sparse to reach any statistically significant conclusions, scaling relations of galaxy luminosities with internal kinematics lead to a second formula for the minimum group velocity dispersion that turns out to be a good predictor, in a statistical sense, of the group velocity dispersion. Only 3 groups (HCG 38, 47 and 88) have statistically significant low velocity dispersions. Finally, analyzing the few compact groups with more secure velocity dispersions obtained through the inclusion of faint galaxies and the immediate group environment, leads to the conclusion that at least one-quarter of Hickson compact groups (including HCG 22, 42, and 88) have significantly low velocity dispersions, meaning that they are either caused by chance alignments of galaxies along the line of sight or alternatively in their final stages of coalescence.

1 Introduction

The nature of the compact groups of galaxies (HCGs) cataloged by Hickson [1] has been a matter of debate for quite some time. If HCGs are as dense in 3D as they appear in projection, their average mass densities would correspond to roughly 10^5 times the mean density of an $\Omega = 0.3$ Universe. If they formed with the same radii as they presently have, their formation redshift would be as high as $z \simeq 8$, at which epoch their galaxies would not yet have been formed! It is unlikely that such groups can survive galaxy mergers within them [2], nor could the groups survive coalescence into larger systems.

The simplest alternative is that compact groups are caused by chance alignments of galaxies along the line-of-sight, within larger groups [3,4], clusters [4,5] or cosmological filaments. [6] Now loose groups (except those found with Friends-of-Friends algorithms[a]) typically have low velocity dispersions, with median values around $100\,\mathrm{km\,s^{-1}}$, while HCGs have median velocity dispersions of order $200\,\mathrm{km\,s^{-1}}$. Hence, those HCGs that have low velocity dispersions are easily understood as chance alignments within loose groups. Alternatively, low group velocity dispersion can be caused by dynamical friction transferring the orbital energy of the group into the internal energy of a single merger remnant.

In this proceeding, I propose a new formalism to disentangle true systems from chance alignments, by asking myself, *what is the minimum velocity dispersion of a spherical dynamical system?* The method is given in Sec. 2, caveats are presented in Sec. 3, and the method is applied to Hickson's compact groups in Sec. 4.

2 Method

2.1 Basic formalism

For near spherical virialized systems, mass increases with some power (near 3, as is easily shown by combining the virial theorem with a critical mean density for virialization) of the velocity dispersion of virialized systems. One therefore expects that there must be a minimum velocity dispersion for a virialized galaxy system to be more massive than the sum of the masses of its member galaxies.

One can obtain a stricter criterion, by also counting the mass in the group that may be beyond the limits (say the virial radii) of its galaxies. Indeed, within a given radius R of the group center, the sum of the masses of the galaxies must be smaller or equal to the mass of the whole group *within the same radius.*

A simpler version of this argument applies for galaxies that lie close to the group center, *i.e.,* forming a sub-system with size

$$R \ll R_{\rm vir} \ , \tag{1}$$

where $R_{\rm vir}$ is the radius within which the mean density is typically 200 times larger than the mean density of the Universe, and within which the group should be in virial equilibrium. Then to first order, the assumed spherically symmetric mass profile of the group should be greater than the sum of the assumed spherically symmetric mass profiles of the galaxies:

$$M(R) \geq \sum_j m_j(R) \ . \tag{2}$$

At radius R, the mass interior to the group follows

$$\begin{aligned} M(R) &= \frac{R}{G} V_{\rm vir}^2 \, \mu(R/R_{\rm vir}) & (3)\\ &= \frac{R}{G} \sigma_v^2 \left(\frac{V_{\rm vir}}{\sigma_v}\right)^2 \mu\left(R/R_{\rm vir}\right) \ , & (4) \end{aligned}$$

where μ is the dimensionless mass profile, $V_{\rm vir}$ is the circular velocity of the virialized group at radius $R_{\rm vir}$, σ_v is the group line-of-sight velocity dispersion, measured by an observer, *i.e.,* the rms velocity dispersion within a circular aperture centered on the group, and G is the gravitational constant.

[a] Loose groups selected with Friends-of-Friends algorithms tend to have velocity dispersions twice as high as groups selected with global algorithms. This occurs because percolation methods applied to small systems of order 10 members tend to return very elongated prolate structures, where the outer members are in fact outliers.

At large radii from the center of an elliptical galaxy j, the interior mass is

$$\begin{aligned} m_j(R) &= \frac{R}{G} v_{\mathrm{vir},j}^2 \, \mu(R/r_{\mathrm{vir},j}) \\ &= \frac{R}{G} \sigma_{v,j}^2 \left(\frac{v_{\mathrm{vir}}}{\sigma_{v,j}}\right)_j^2 \mu\left(R/r_{\mathrm{vir},j}\right) \ , \end{aligned} \tag{5}$$

where again μ is the dimensionless mass profile and $v_{\mathrm{vir},j}$ is the circular velocity at radius $r_{\mathrm{vir},j}$, within which the galaxy is expected to be virialized.[b] Here again, $\sigma_{v,j}$ is the aperture rms velocity dispersion, as would be measured by an observer.

Similarly, at large radii from the center of disk galaxy j, with deprojected maximum rotation velocity $v_{\mathrm{rot},j}$, where the visible matter becomes negligible, one can write its mass as

$$m_j(R) = \frac{R}{G} v_{\mathrm{rot},j}^2 \left(\frac{v_{\mathrm{vir}}}{v_{\mathrm{rot},j}}\right)^2 \mu\left(R/r_{\mathrm{vir},j}\right) \ , \tag{6}$$

with similar notations.

Since the group is more massive than *any* of its galaxies, one expects $R_{\mathrm{vir}} > r_{\mathrm{vir},j}$, hence $\mu(R/R_{\mathrm{vir}}) < \mu(R/r_{\mathrm{vir},j})$. Therefore, given Eqs. (4) and (6), and that the velocity dispersion at group collapse is larger (though similar) to the velocity dispersion it will have at virialization, then Eq. (2) implies

$$\begin{aligned} \sigma_v^2 &\geq \left(\frac{\sigma_v}{V_{\mathrm{vir}}}\right)^2 \\ &\times \left[\left(\frac{v_{\mathrm{vir}}}{\sigma_{v,j}}\right)^2 \sum_E \sigma_{v,j}^2 + \left(\frac{v_{\mathrm{vir}}}{v_{\mathrm{rot}}}\right)^2 \sum_D v_{\mathrm{rot},j}^2\right] \ , \end{aligned} \tag{7}$$

where the sums are over ellipticals (E) and disks, *i.e.*, spirals and lenticulars, (D).

2.2 Scaling with the NFW profile

I now evaluate the terms in parentheses in Eq. (7). For example, if galaxy halos and virialized groups both had singular isothermal profiles $\rho \sim r^{-2}$, then $\sigma_v = 2^{-1/2} V_{\mathrm{vir}}$ and the galaxies would have constant deprojected rotation velocity equal to $v_{\mathrm{vir},j}$. Then, Eq. (7) would lead to the simple relation

$$\sigma_v^2 \geq \sum_E \sigma_v^2(0) + \frac{1}{2} \sum_D v_{\mathrm{rot}}^2 \ . \tag{8}$$

Recent cosmological simulations show a varying slope in the density profile of dark matter halos. In particular, halos in high resolution cosmological simulations follow extremely well[7] the universal density profile first proposed by Navarro et al. [8], and hereafter denoted NFW profile, whose slope varies from -1 in the core to -3 in the envelope:

$$\rho(r) \sim r^{-1} (r+a)^{-2} \ . \tag{9}$$

Moreover, the profiles are nearly self-similar for different masses and initial conditions [7], as the *concentration parameter* $c = R_{\mathrm{vir}}/a$, varies slowly with mass within the virial radius, $M_{\mathrm{vir}} = M(R_{\mathrm{vir}})$.[c] From Fig. 6 of Navarro et al. [7], I infer concentration parameters

$$c = \begin{cases} 15\left(h M_{\mathrm{vir}}/10^{12} M_\odot\right)^{-0.12} \ (\mathrm{SCDM}) \\ 11\left(h M_{\mathrm{vir}}/10^{12} M_\odot\right)^{-0.11} \ (\Lambda\mathrm{CDM}) \end{cases} \ , \tag{10}$$

[b] Uppercase R, V and M are used for groups and lowercase for galaxies.

[c] M_{vir}, the mass within the virial radius, should not be confused with the virial mass estimate!

where $h = H_0/\left(100\,\mathrm{km\,s^{-1}\,Mpc^{-1}}\right)$. Here and below, SCDM and ΛCDM refer to the CDM cosmologies, with contributions to Ω from matter and the cosmological constant respectively equal to ($\Omega_M = 1$, $\Omega_\Lambda = 0$) for SCDM and ($\Omega_M = 0.3$, $\Omega_\Lambda = 0.7$) for ΛCDM.

For elliptical galaxies with $m_{\rm vir} \geq 10^{11} h^{-1} M_\odot$, *i.e.*, $c < 19.8$ (SCDM) and 14.2 (ΛCDM), the aperture velocity dispersion satisfies [9]

$$\frac{v_{\rm vir}}{\sigma_v(r)} \geq \begin{cases} 1.10 & \text{(SCDM)} \\ 1.20 & (\Lambda\text{CDM}) \end{cases} \quad \forall r \ , \tag{11}$$

where the equality is reached at $m_{\rm vir} = 10^{11} h^{-1} M_\odot$, and where the dependence on cosmology comes from the different concentration parameters for given mass (Eq. 10). Note that the velocity dispersion measured by observers can be measured in a small or large aperture, as Eq. (11) is valid at all radii.

For disk galaxies with $m_{\rm vir} \geq 10^{11} h^{-1} M_\odot$, one can solve for the circular velocity (with eq. [5] of Navarro et al. [10]), to obtain $(v_{\rm circ}^{\rm max}/v_{\rm vir})^2 \simeq 0.216\, c/f(c)$ [11], where $f(x) = \ln(1+x) - x/(1+x)$. This yields

$$\frac{v_{\rm circ}}{v_{\rm vir}} \leq \begin{cases} 1.43 & \text{(SCDM)} \\ 1.31 & (\Lambda\text{CDM}) \end{cases} \quad \forall r \ , \tag{12}$$

where $v_{\rm vir}$ is the circular velocity at radius $r_{\rm vir}$ and the equality is reached for $m_{\rm vir} = 10^{11} h^{-1} M_\odot$. In Eq. (12), $v_{\rm circ}$ corresponds to the circular velocity of the halo, whereas observers measure the total rotation of the galaxy, to which the halo contributes only a fraction $f_{\rm halo} \leq 1$. We infer that

$$f_{\rm halo} = \frac{v_{\rm circ}}{v_{\rm rot}} \gtrsim 0.8 \tag{13}$$

from Kent's [12]'s decomposition of spiral rotation curves into disk, bulge, and halo components.[d] Therefore,

$$\frac{v_{\rm vir}}{v_{\rm rot}} > \begin{cases} 0.56 & \text{(SCDM)} \\ 0.61 & (\Lambda\text{CDM}) \end{cases} \ . \tag{14}$$

For the group itself, assuming a mass $M_{\rm vir} < 3 \times 10^{13}\, h^{-1}\, M_\odot$, for which, according to Eq. (10) $c > 10.0$ (SCDM) and 7.6 (ΛCDM), the aperture rms velocity dispersion obeys

$$\frac{\sigma_v(R)}{V_{\rm vir}} \geq \begin{cases} 0.66 & \text{for } 0.010 < R/R_{\rm vir} < 1 \quad \text{(SCDM)} \\ 0.64 & \text{for } 0.015 < R/R_{\rm vir} < 1 \quad (\Lambda\text{CDM}) \end{cases} \ , \tag{15}$$

where the equalities are for $R = R_{\rm vir}$. Note that the velocity dispersions of groups are always estimated by observers within the large range of applicability of the inequalities of Eq. (15).

Combining Eqs. (7), (11), (14) and (15), I finally obtain

$$\begin{aligned} \sigma_v &\geq \sigma_v^{\rm min,kin} \\ \left(\sigma_v^{\rm min,kin}\right)^2 &= \begin{cases} 0.53 \sum_E \sigma_{v,j}^2(0) + 0.14 \sum_D v_{{\rm rot},j}^2 & \text{(SCDM)} \\ 0.59 \sum_E \sigma_{v,j}^2(0) + 0.15 \sum_D v_{{\rm rot},j}^2 & (\Lambda\text{CDM}) \end{cases} \end{aligned} \tag{16}$$

2.3 Extension to photometric data with galaxy scaling relations

When internal kinematical data on galaxies is unavailable, one can resort to scaling relations to guess the maximum rotation velocities of disks and velocity dispersions of bulges.

For bulge-dominated galaxies, I adopt the renormalized [13] Faber-Jackson [14] relation:

$$M_B - 5\,\log h = -A - 9\,(\log \sigma_v - 2.3) \ , \tag{17}$$

[d] Note that Kent's [12] decomposition is based upon halos with flat inner cores, contrary to the the NFW profile.

where $A = 19.4$ for ellipticals and $A = 19.6$ for lenticulars. Note that if surface photometry is available one can get much more precise measures of the velocity dispersion with the Fundamental Plane scalings.

For disk-dominated galaxies, I adopt the Tully-Fisher [15] relation, with zero-points from the recent analysis of Sakai et al. [16], who determined distances to their galaxies using Cepheids observed with the HST:

$$M_B = -7.85 \left(\log W_{20}^c - 2.5\right) - 19.7 \ , \tag{18}$$

where M_B is the extrapolated total absolute magnitude of the galaxy, after correction for internal and Galactic extinction, and W_{20}^c is the line-width of the 21 cm line, measured at 20% maximum (or 20% of the mean of the two peaks for double horned profiles), and corrected for inclination and redshift. Sakai et al. [16] also mention that the W_{20}^c is 10% larger than the 50% width, which after correction for inclination and redshift corresponds to twice the maximum rotation velocity. Thus,

$$v_{\rm rot} = \frac{W_{20}^c}{2.2} \ . \tag{19}$$

Inserting Eqs. (17), (18) and (19) into Eq. (16), and adopting $h = 0.7$, one then obtains

$$\begin{aligned}
\sigma_v &\geq \sigma_v^{\min,L} \\
\left(\frac{\sigma_v^{\min,L}}{100\,\rm km\,s^{-1}}\right)^2 &= 2.1 \sum_E {\rm dex}[-(M_B+20)/4.5] \\
&+ 1.9 \sum_L {\rm dex}[-(M_B+20)/4.5] \\
&+ 0.4 \sum_S {\rm dex}[-(M_B+20)/3.9] \ ,
\end{aligned} \tag{20}$$

where the sums are over ellipticals, lenticulars and spirals, respectively. Eq. (20) is scaled to the ΛCDM cosmology, while the SCDM cosmology would yield values $\simeq 5\%$ lower in $\sigma_v^{\min,L}$ (see Eq. [16]). Note that with $h = 0.7$, $M_B = -20$ corresponds to $L \simeq 0.65\,L_*$.

3 Caveats

Any radius R can be used in the analysis of Sec. 2.1, as long as it is much larger than the typical separations between the galaxies. The assumption of universal (although not self-similar) NFW mass profiles, can be extended to the distribution of matter *beyond the virial radii* of cosmic structures (where $\mu > 1$). Indeed, high resolution cosmological simulations show that the density profile obeys *on average* the NFW model out to $> 1.5\,R_{\rm vir}$ [17,18]). Note, however, that the density profiles obtained from cosmological simulations display considerable scatter [19,11] and the outer slopes of galaxy halos within groups are shallower (-2.5) than the NFW slope of -3 [19]. Moreover, while halos are near spherical (short to long axis ratio $\simeq 2/3$) within $R_{\rm vir}$ [20], they become somewhat flatter outside of $R_{\rm vir}$. Therefore, our assumption of spherical symmetry really holds best within $R_{\rm vir}$.

Moreover, the inner -1 slope of the NFW density profile used in Sec. 2.2 is still under debate as various authors [21,22,23,24] are claiming density profiles scaling as $R^{-1.5}$ in the inner regions.

The cuspy -1 or -1.5 inner halo slopes seen in the simulations may very well be unrealistic on the scales of galaxies, as they conflict with spiral galaxy rotation curves [25]. One must hope that the gas in galaxies settles in the center with a homogeneous core, and that in turn this homogeneous gas core, though gravitational interactions forces the dark matter to have a fairly shallow inner density profile. The precise inner density profile of spiral galaxies is unimportant for the present study, except in understanding the measurement of maximum velocity, *i.e.,* the evaluation of $f_{\rm halo}$ (Eq. [13]).

When galaxies interact, some matter moves out in tidal tails to large radii. Therefore, underlying the analysis of Sec. 2.1 are the (reasonable) assumptions that 1) the measurements of the internal kinematics of galaxies are unaffected by the escape of this matter (if anything, matter removed from the inner regions of galaxies leads to an underestimate of the depth of the potential well of a galaxy within a group), and 2) the fraction of matter escaping the group altogether is negligible. In essence, I am actually comparing the mass profile of the group with the sum of the mass profiles of its galaxies *had they not assembled (and mixed, with their outer regions tidally shorn) inside the group, but remain isolated instead.*

Galaxies outside the group core can be included in Eq. (16), but with a weighting factor between 1/2 and unity on squared rotational velocity or velocity dispersion, to avoid accounting for the mass outside of the group.

One may worry that the presence of a central massive black hole in an elliptical galaxy or spiral bulge may lead one to overestimate the galaxy's internal velocity dispersion. However, given that black holes appear to account for a fraction $\epsilon = 0.6\%$ of the mass of ellipticals and bulges [26]), their effect is small on the scales where observers measure the velocity dispersion. Indeed, since the black hole mass $m_{\rm BH}$ satisfies

$$m_{\rm BH} = \epsilon \left(\frac{M}{L}\right) L < \epsilon\, m_{\rm vir} \ ,$$

where L is the galaxy luminosity, then for $m_{\rm BH} \ll M(R)$, one needs to check that the fraction of the galaxy's mass at radius R is much larger than ϵ:

$$\frac{m(R)}{m_{\rm vir}} = \frac{f(R/r_{\rm vir})}{f(c)} \gg \epsilon \ . \tag{21}$$

Given a galaxy mass $m_{\rm vir}$, one derives c from Eq. (10) and $r_{\rm vir}$ from the fact that the galaxy's mean density within $r_{\rm vir}$ is Δ times the mean density of the Universe:

$$\frac{3 m_{\rm vir}}{4\pi r_{\rm vir}^3} = \Omega_M \Delta \left(\frac{3H_0^2}{8\pi G}\right) \ . \tag{22}$$

Adopting

$$\Delta = \left\{ \begin{array}{ll} 18\,\pi^2 = 178 & \text{(SCDM)} \\ 334 & (\Lambda\text{CDM}) \end{array} \right. \ , \tag{23}$$

where the latter term is obtained from Eq. [A5] of Kitayama & Suto [27]. One finds that for galaxies with $m_{\rm vir} < 5\times 10^{12} h^{-1} M_\odot$ as close as $10\,h^{-1}$ Mpc, where $1''$ subtends only 50 pc, the mass fraction within $1''$ is always greater than 28% (SCDM) and 19% (ΛCDM). Hence Eq. (21) is satisfied and the central black hole contributes negligibly to the observed aperture rms velocity dispersion of ellipticals.

One should avoid the temptation of adding the separate bulge and disk contributions to the minimum group velocity dispersion, since the internal kinematics of both components are tracing the same overall gravitational potential (albeit in different regions of the galaxy). Which component should then be used? I use the component that contributes the most to the minimum velocity dispersion of the group, i.e., from Eq. (16), the disk if $v_{\rm rot} \geq 2\,\sigma_v^{\rm bulge}$ and the bulge otherwise.

For highly evolved isolated galaxy systems, where galaxies are undergoing collective coalescence, *tidal friction* will transfer important fractions of the orbital energy into internal motions in the galaxies, and in the limit of coalescence, the galaxy system will have zero velocity dispersion. Such collective coalescence is expected to be rare, although HCG 79, as well as one (non-Hickson) low velocity dispersion compact group of galaxies [28] do show this phenomenon. In general, galaxy merging in groups will proceed hierarchically, and the net effect of tidal friction will be small, though non-negligible.

The minimum velocity dispersion applies also to groups that are non-fully virialized, but whose components are near or past full cosmological collapse. Indeed, at collapse the orbital velocities of the galaxies must be larger than at virialization.

Finally, the minimum velocity dispersions (Eqs. [16] and [20]) cannot be applied to individual groups, because the group velocity dispersion, measured with the standard deviation of typically 4 radial velocities, is too noisy. It only makes sense to apply this criterion statistically to sets of groups.

4 Application to Hickson compact groups

I now apply the minimum velocity dispersion criteria of Sec. 2.1 to Hickson's [1] well-studied catalog of compact groups of galaxies. HCGs have the advantage that their galaxies are chosen with a very high equivalent density threshold, combined with an isolation criterion, such that the galaxies lie well within the virial radius (Eq. [1]). Indeed, the median galaxy separation within HCGs is $39\,h^{-1}\,\mathrm{kpc}$ [29]. The virial radius is easily obtained as a function of measured group velocity dispersion. The mean density within the virial radius can be written as Δ times the mean density of the Universe, *i.e.*,

$$\frac{3M_{\rm vir}}{4\pi R_{\rm vir}^3} = \frac{3H_0^2\Omega_0\Delta}{8\pi G} \ . \tag{24}$$

Moreover, the aperture rms velocity dispersion satisfies

$$\sigma_v = \alpha\, V_{\rm vir} \ , \tag{25}$$

with

$$\alpha < \left\{ \begin{array}{ll} 0.85 & \mathrm{(SCDM)} \\ 0.78 & (\Lambda\mathrm{CDM}) \end{array} \right. \ , \tag{26}$$

for all apertures when $M_{\rm vir} > 10^{12} h^{-1} M_\odot$, *i.e.*, concentration parameters smaller than $c = 15$ and 11, for SCDM and ΛCDM respectively, according to Eq. (10). Combining Eqs. (23), (24), (25) and (26), the virial radius satisfies

$$R_{\rm vir} > R_1 \left(\frac{\sigma_v}{200\,\mathrm{km\,s^{-1}}}\right) \ , \tag{27}$$

where

$$hR_1 < \left\{ \begin{array}{ll} 249\,\mathrm{kpc} & \mathrm{(SCDM)} \\ 362\,\mathrm{kpc} & (\Lambda\mathrm{CDM}) \end{array} \right. \ . \tag{28}$$

Given that the median velocity dispersion of HCGs is $200\,\mathrm{km\,s^{-1}}$ [29], one sees that the median radial separation is 6 (SCDM) to 9 (ΛCDM) times lower than $R_{\rm vir}$. Hence the formalism of Sec. 2.1 applies to HCGs.

4.1 Internal kinematics of original HCG galaxies

Table 1 below displays all known kinematic information for HCG accordant redshift galaxies, whose parent HCGs have at least 3 accordant redshifts. Galaxies with rotation curves with sinusoidal radial variations or with one side of the major axis with negligible velocities (at least within their inner regions) are omitted. HCG 18 and 54 also omitted, as there is strong suspicion that these systems are single galaxies rather than groups.[30] When the two sides of a spiral have maximum rotation velocities that agree to within 30%, the arithmetic mean is given. When kinematic data for a given galaxy is available from different authors, both are shown, unless one is performed with two-dimensional spectroscopy [31,32] in which case the other (slit spectroscopy) measurement is discarded. If two measurements of a given galaxy are slit-based, then the arithmetic mean is adopted if the two agree to better than 30%.

Table 2, which lists the minimum (Eq. [16], assuming ΛCDM, while SCDM values are 5% lower) and measured [29] velocity dispersions for HCGs with at least two galaxies with measured internal kinematics. The measured (one-dimensional) velocity dispersions use the formula

$$\sigma_v^2 = \frac{n}{n-1} \left(\left\langle v^2 \right\rangle - \langle v \rangle^2\right) - \left\langle (\delta v)^2 \right\rangle \ , \tag{29}$$

Although a small fraction of HCGs display *some* internal kinematics data, Table 2 shows that 10 HCGs out of 20 have velocity dispersions lower than $\sigma_v^{\rm min,kin}$, with 4 of these (HCGs 68, 88, 89, and 90) with velocity dispersions lower than $0.65\,\sigma_v^{\rm min}$.

However, the wide dispersion in measured standard deviations can give the illusion of a large proportion of low velocity dispersions. In other words, the high fraction of low velocity dispersion HCGs may be caused by tangential motions within moderate or high true velocity dispersion groups.

One can quantify this effect analytically for a set of groups with the same number n of galaxies. Indeed, if σ_v^2 is the sample variance, while $\widetilde{\sigma}_v^2$ is the true variance, then it is known that $(n-1)\sigma_v^2/\widetilde{\sigma}_v^2$ follows the χ^2 distribution with $n-1$ degrees of freedom. Most HCGs are quartets, and for $n=4$, the expected fraction of quartets with $\sigma_v < 0.6\,\widetilde{\sigma}_v$ is $P(\chi_3^2 < 3 \times [0.65]^2) = 0.26$. The generalization to handle the errors in the velocity measurements is straightforward, but yields very similar results as the velocity errors are typically much smaller than the measured velocity dispersions.

The generalization to a set of groups with different multiplicities is difficult, but can be performed with Monte-Carlo simulations. For this, I generate groups of n points, and attribute them velocities from a gaussian distribution of zero mean and unit standard deviation. The distribution of n is taken from the HCG catalog. I iterate this procedure 1000 times, yielding 90000 simulated groups. Note that I do not implement the selection criterion that all HCG galaxies have velocities within $1000\,\rm km\,s^{-1}$ from the group median, hence we will very slightly overestimate the fraction of groups with very high $\sigma_v/\sigma_v^{\rm true}$.

The Monte-Carlo simulations confirm that 28% of the time, the group velocity dispersion will be measured to be less than 65% of its true velocity dispersion. So if we equate, in a null hypothesis, the true group velocity dispersion with $\sigma_v^{\rm min}$, the observation of 4 groups out of 20 with velocity dispersions less than 65% of the minimum allowed dispersion is roughly what is expected.

4.2 Luminosities of original HCG groups

For better statistics, I now apply the minimum velocity dispersions from the luminosities of the galaxies (eq. [20]), as these are known for *all* HCGs. Figure 1 displays the distribution of $\sigma_v/\sigma_v^{\rm min}$ for the 90 accordant redshift (without HCG 18 and 54, deemed to be single galaxies) HCGs (using eq. [20]), together with the prediction from the Monte-Carlo simulations, in the null hypothesis that each group has a true velocity dispersion equal to $\sigma_v^{\rm min}$.

The general agreement between the observed distribution of minimum velocity dispersion ratios and expected velocity dispersion ratios, assuming all groups are real and that all mass is accounted for is remarkable. This agreement suggests that indeed nearly all the mass in groups is accounted for by the bright galaxies, with negligible mass in fainter galaxies, as well as a smoothly distributed intergalactic medium, both dark matter and hot gas. Again, as

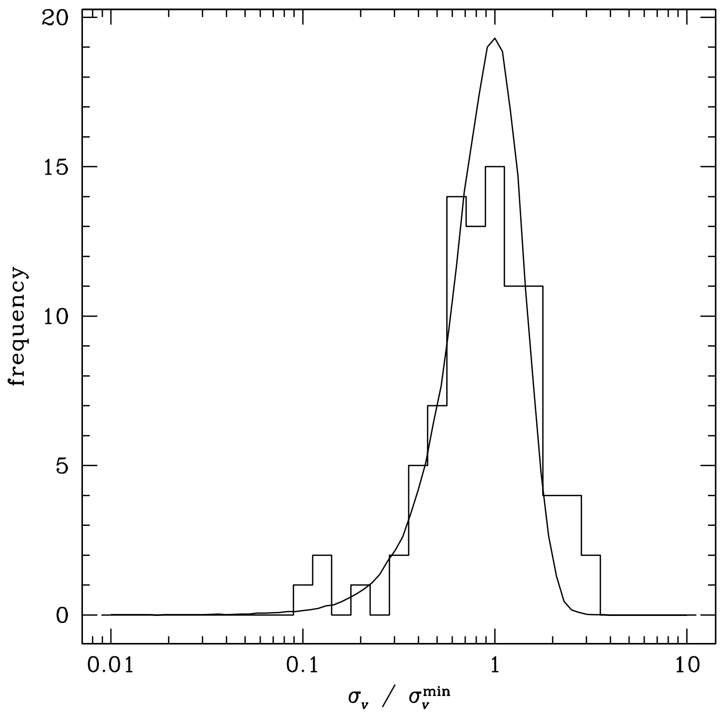

Figure 1: *Histogram*: distribution of $\sigma_v/\sigma_v^{\mathrm{min},L}$ for 90 HCGs with at least 3 accordant redshifts (groups HCG 18 and 54 were omitted, as they are deemed to be single galaxies). *Curve:* distribution predicted from Monte-Carlo simulations, assuming that the true velocity dispersion is $\sigma_v^{\mathrm{min},L}$ (taken from Eq. [20]).

mentioned in Sec. 3, the total mass in galaxies is understood to represent the galaxies had they not assembled into a compact group, but remained isolated instead.

The two distributions in Figure 1 are fairly similar, with an excess of 3 very low velocity dispersion groups: HCGs 38, 47, and 88. The excess of 5 very high velocity dispersion groups (HCGs 14, 48, 71, 80 et 82) suggests that either these are contaminated by interlopers or have a substantial fraction of mass between the bright galaxies.

4.3 Luminosities of HCG groups, expanded to larger sizes and fainter galaxies

Since the measured velocity dispersions are uncertain, given the small numbers (typically 4) of velocities used in each group to measure them, I now attempt to make use of HCGs defined in a larger sense:

Table 3 lists all HCGs in which spectra were systematically measured for fainter members and for the immediate environment by de Carvalho et al. [41] and Zabludoff & Mulchaey. [42]

5 Discussion

If one does not wish to be swamped by small number statistics, one needs to apply the formalism of minimum group velocity dispersions to groups extended to faint members and their immediate surroundings, and apply the luminosity scaling relations to infer statistically the internal kinematics of the galaxies. When this is done, roughly one-quarter of HCGs with spectroscopy extended to faint members and their immediate environments show abnormally low velocity dispersions, when much fewer low velocity dispersion groups are expected on statistical grounds.

Two very different scenarios can lead to such low velocity dispersion compact groups. One is that the compact groups arise as chance alignments of galaxies along the line of sight within larger structures (loose groups [3], clusters [4], and cosmological filaments [6]).

Alternatively, low velocity dispersion compact groups may simply be in their final stages of coalescence, with efficient transfer of the group orbital energy into the internal energies of the merging clumps, or in another words, efficient dynamical friction felt by the galaxies about to merge.

The coalescing scenario is favored in unusually compact groups with highly disturbed galaxies, such as HCG 79 (Seyfert's Sextet) and HCG 88, as well as a coalescing non-Hickson compact group discovered recently. [28]

In any event, the remarkable match between the observed velocity dispersions and minimal theoretical velocity dispersions suggests that most of the group mass is in the bright galaxies (and their halos), and little is in the form of fainter galaxies or a smooth background. Since many compact groups have a smooth X-ray intra-group medium, it appears that this X-ray plasma originates from tidal truncation of the galaxies during the assembly of the compact group.

Acknowledgments

I am grateful to Sergio Dos Santos, Trevor Ponman and Duncan Forbes for useful discussions.

References

1. Hickson, P., 1982, ApJ 255, 382
2. Mamon, G.A., 1987, ApJ 321, 622
3. Mamon, G.A., 1986, ApJ 307, 426
4. Walke, D.G., Mamon, G.A., 1989, A&A 225, 291
5. Mamon, G.A., 1989, A&A 219, 98
6. Hernquist, L., Katz, N., Weinberg, D.H., 1995, ApJ 442, 57
7. Navarro, J.F., Frenk, C.S., White, S.D.M., 1997, ApJ 490, 493
8. Navarro, J.F., Frenk, C.S., White, S.D.M., 1995, MNRAS 275, 720
9. Łokas, E.L., Mamon, G.A., 2000, MNRAS in press, astro-ph/0002395
10. Navarro, J.F., Frenk, C.S., White, S.D.M., 1996, ApJ 462, 563
11. Bullock, J.S., Kolatt, T.S., Sigad, Y., Somerville, R.S., Kravtsov, A.V., Klypin, A.A., Primack, J.R., Dekel, A., 1999, MNRAS submitted, astro-ph/9908159
12. Kent, S.M., 1987, AJ 93, 816
13. de Vaucouleurs, G., Olson, D.W., 1982, ApJ 256, 346
14. Faber, S.M., Jackson, R.E., 1976, ApJ 204, 668
15. Tully, R.B., Fisher, J.R., 1977, A&A 54, 661
16. Sakai, S., Mould, J.R., Hughes, S.M.G., Huchra, J.P., Macri, L.M., Kenicutt, R.C., Gibson, B.K., Ferrarese, L., Freedman, W.L., Han, M., Ford, H.C., Graham, J.A., Illingworth, G.D., Kelson, D.D., Madore, B.F., Sebo, K., Silbermann, N.A., Stetson, P, B., 2000, ApJ 529, 698
17. Huss, A., Jain, B., Steinmetz, M., 1999, ApJ 517, 64
18. Jing, Y.P., 2000, ApJ 535, 30
19. Avila-Reese, V., Firmani, C., Klypin, A., Kravtsov, A.V., 1999, MNRAS 310, 527
20. Cole, S., Lacey, C., 1996, MNRAS 281, 716
21. Fukushige, T., Makino, J., 1997, ApJ 477, L9
22. Moore, B., Governato, F., Quinn, T., Stadel, J., Lake, G., 1998, ApJ 499, L5
23. Moore, B., Quinn, T., Governato, F., Stadel, J., Lake, G., 1999, MNRAS 310, 1147
24. Jing, Y.P., Suto, Y., 2000, ApJ 529, L69

25. Flores, R.A., Primack, J.R., 1994, ApJ 427, L1
26. Magorrian, J., Tremaine, S., Richstone, D., Bender, R., Bower, G., Dressler, A., Faber, S.M., Gebhardt, K., Green, R., Grillmair, C., Kormendy, J., Lauer, T., 1998, AJ 115, 2285
27. Kitayama, T., Suto, Y., 1996, ApJ 469, 480
28. Weinberger, R., Temporin, S., Kerber, F., 1999, ApJ 522, L17
29. Hickson, P., Mendes de Oliveira, C., Huchra, J.P., Palumbo, G.G., 1992, ApJ 399, 353
30. Plana, H., Amram, P., Mendes de Oliveira, C., Balkowski, C., 2000, AJ 120, 621
31. Mendes de Oliveira, C., Plana, H., Amram, P., Bolte, M., Boulesteix, J., 1998, ApJ 507, 691
32. Plana, H., Mendes de Oliveira, C., Amram, P., Boulesteix, J., 1998, AJ 116, 2123
33. Bonfanti, P., Simien, F., Rampazzo, R., Prugniel, P., 1999, A&AS 139, 483
34. Longo, G., Busarello, G., Lorenz, H., Richter, G., Zaggia, S., 1994, A&A 282, 418
35. Moles, M., Marquez, I., Sulentic, J.W., 1998, A&A 334, 473
36. Nishiura, S., Shimada, M., Ohyama, Y., Murayama, T., Taniguchi, Y., 2000, AJ 120, 1691
37. Rampazzo, R., Covino, S., Trinchieri, G., Reduzzi, L., 1998, A&A 330, 423
38. Rubin, V.C., Hunter, D.A., Ford, W. Kent, J., 1991, ApJS 76, 153
39. Verdes-Montenegro, L., Del Olmo, A., Perea, J., Athanassoula, E., Marquez, I., Augarde, R., 1997, A&A 321, 409
40. Zepf, S.E., Whitmore, B.C., 1993, ApJ 418, 72
41. de Carvalho, R.R., Ribeiro, A.L.B., Zepf, S.E., 1994, ApJS 93, 47
42. Zabludoff, A.I., Mulchaey, J.S., 1998, ApJ 496, 39

Table 1: HCG internal kinematics

Galaxy	$v_{\rm rot}$	ref.	σ_v	ref.	Galaxy	$v_{\rm rot}$	ref.	σ_v	ref.
7a	243/150	N+00			67a			291	B+99
10b			210	ZW93	67d			112	B+99
14b			125	ZW93	68a			361	R+98
15b			182	ZW93	68b			241	R+98
15c			150	ZW93	68c	214	N+00		
16a	247	MO+98	53	MO+98	74a			312	B+99
16b	192/81	MO+98			74b			212	B+99
16c	257	MO+98	55	MO+98	76b			185	ZW93
16d	105	MO+98	62	MO+98	76c			160	ZW93
22a			207	ZW93	78a	207	RHF91		
23a	261	RHF91			79a			155	B+99
23b	182	RHF91			79b			130	B+99
28b			173	ZW93	79c			59	B+99
32a			146	ZW93	79d	114	RHF91		
33c	237	RHF91			79d	80/48	N+00		
34b	208	RHF91			80a	235/107	N+00		
37a			245	ZW93	86a			232	ZW93
37b	244	RHF91,N+00			86b			189	ZW93
37e			104	ZW93	87a	335	N+00		
38a	165	N+00			87c	228/145	N+00		
40a			199	ZW93	88a	325/249	RHF91,N+00		
40c	220	RHF91, N+00			88d	140	N+00		
40d	200	RHF91			89a	153	RHF91,N+00		
40e	132	RHF91			89b	149	RHF91		
42a			290	ZW93	90a			180	L+94
44a	275	RHF91, N+00			90b	122	P+98	60	P+98
44b			205	ZW93	90c	85	P+98	80	P+98
44c	166	RHF91,N+00			90d	220	P+98	110	P+98
47a	195	N+00			92b	>145	MMS98	220	MMS98
53a	270	N+00			92d			230	MMS98
57b	298	RHF91			92e			215	MMS98
57c			158	ZW93	93c	339/154	N+00		
57d	200	RHF91			96a	200	VM+97		
57e	313	RHF91			96b			200	VM+97
57f			114	ZW93	96c	317	VM+97		
61c	210	N+00			97a			166	ZW93
62a			246	R+98	100a	265/201	RHF91		
62b			272	R+98					

Notes: Columns (1) and (6): HCG galaxy. Columns (2) and (7): maximum deprojected rotation velocity ($\rm km\,s^{-1}$). Columns (3) and (8): reference for rotation velocity. Columns (4) and (9): central velocity dispersion ($\rm km\,s^{-1}$). Columns (5) and (10): reference for velocity dispersion. References: B+99 [33]; L+94 [34]; MMS98 [35]; MO+98 [31]; N+00 [36]; P+98 [32]; R+98 [37]; RHF91 [38]; VM+97 [39]; ZW93 [40].

Table 2: Hickson compact group minimum and observed velocity dispersions

HCG	$N_{\rm disks}$	$N_{\rm bulges}$	$\sigma_v^{\rm min,kin}$ ($\rm km\,s^{-1}$)	N	σ_v ($\rm km\,s^{-1}$)
15	0	2	181	6	462
16[a]	3	1	164, 149	4	139
23	2	0	123	4	187
37	1	2	225	5	443
40	3	1	198	5	163
44	2	1	201	4	148
57	3	2	238	7	284
62	0	2	282	4	329
67	0	2	240	4	240
68	1	2	344	5	169
74	0	2	290	5	350
76	0	2	188	7	258
79[b]	1	3	163 – 168	4	156
86	0	2	230	4	307
87[c]	2	0	141, 157	3	119
88[d]	2	0	57, 111	4	0[e]
89	2	0	83	4	44
90	2	2	180	4	111
92	0	3	295	4	450
96	2	1	211	4	148

Columns (2) and (3): number of spirals and bulges/ellipticals used; column (4) minimum group velocity dispersion for ΛCDM (Eq. [16]); column (5) number of accordant redshift galaxies in group; column (6) measured [29] group velocity dispersion ($\rm km\,s^{-1}$, using Eq. [29]). a) The two values of $\sigma_v^{\rm min,kin}$ for HCG 16 correspond to the two choices of $v_{\rm rot}^{\rm max}$ for galaxy 16b. b) The range of values of $\sigma_v^{\rm min,kin}$ for HCG 79 correspond to the three choices of $v_{\rm rot}^{\rm max}$ for galaxy 79d. c) The two values of $\sigma_v^{\rm min,kin}$ for HCG 87 correspond to the two choices of $v_{\rm rot}^{\rm max}$ for galaxy 87c. d) The two values of $\sigma_v^{\rm min,kin}$ for HCG 88 correspond to the two choices of $v_{\rm rot}^{\rm max}$ for galaxy 88a. e) The velocity dispersion of HCG 88 is 0 because the rms velocity error is greater than the standard deviation of the velocities. The maximum likelihood estimate of its velocity dispersion is $16\,\rm km\,s^{-1}$.

Table 3: Extended HCGs

HCG	N_z	σ_v (km s^{-1})	$\sigma_v^{\min,L}$ (km s^{-1})	$P(\sigma_v < \sigma_v^{\min,L})$
4	4	612	222	1
16	7	73	152	0.048
19	5	53	133	0.061
22	4	35	185	0.014
23	7	333	137	1
40	7	294	275	0.76
42	22	211	324	0.014
62	45	376	264	1
63	6	168	155	0.78
64	6	232	149	0.99
67	14	344	317	0.78
86	17	438	306	1
87	6	227	198	0.84
88	6	27	173	0.00041
90	16	193	238	0.21
97	14	409	258	1

Column (1): HCG. Column (2): number of galaxies with accordant redshifts (including environment and faint members). Column (3) velocity dispersion (including environment and faint members). Column (4): minimum velocity dispersion (Eq. [20]). Column (5); probability that $\sigma_v < \sigma_v^{\min,L}$.